

Comparative Study Between Mdct in Chest and Brain Ct Scan by Dose and Image Quality Parameters

Masar Ali Obeed^{1*}, Rasha Sabeeh Ahmed², Mohammed Bader Hassan³

^{1,2}Department of Physiology and Medical Physics, College of Medicine, Al-Nahrain University, Baghdad, Iraq.

³College of Medicine, Al- Iraqia University, Baghdad, Iraq

*Correspondence author: Masar Ali Obeed

Received: 10 January 2023

Accepted: 3 April 2023

Citation: Obeed MA, Ahmed RS, Hassan MB (2023) Comparative Study Between Mdct in Chest and Brain Ct Scan by Dose and Image Quality Parameters History of Medicine 9(1): 2414–2420. <https://doi.org/10.17720/2409-5834.v9.1.2023.312>

Abstract

Background: Multidetector computed tomography (MDCT) has become a routine imaging modality for numerous clinical applications due to its extensive availability, reduced invasiveness, rapid scanning time, great anatomical resolution, and superior diagnostic value. At the same time, the radiation dose to the patient and the concern surrounding this problem has also increased. **Objective:** The aim of this study is to assess image quality related to patient radiation dose for multidetector computed tomography in chest and brain CT examinations. **Patients and Methods:** A total of 60 patients who underwent chest and brain scans from four hospitals on 16, 32, and 64 slice (CT) scanners. Clinical image data were used for image quality calculation and dose assessment. The image quality is calculated by CNR & SNR. The CT dose volume index (CTDI_v) and dose length product (DLP) were documented from the image display. **Results:** Regarding the radiographic parameters, the mean value of radiation doses (CTDI_v, DLP and ED) to patients were higher from 64 slice scanner for the chest CT scan examination (12.6 ± 0.21 , 478.6 ± 73.3 and 6.7 ± 1.026) respectively. It was significantly lower in 32 and 16 slice multi detector CT (9.34 ± 0.23 , 341.86 ± 11.56 and 4.78 ± 0.164) (7.6 ± 1.5 , 247.9 ± 52.6 and 3.46 ± 0.738) respectively. the same parameters in brain CT scan examinations, the mean value of radiation doses (CTDI_v, DLP and ED) to patients were higher from 64 slice scanner (79.75 ± 1.69 , 1598.8 ± 110.8 and 3.35 ± 0.23) respectively. It was significantly lower in 32 and 16 slice multi detector CT (69.54 ± 4.74 , 986.9 ± 72.17 and 2.07 ± 0.15) (54.21 , 943.8 ± 21.74 , and 1.98 ± 0.045) respectively. Regarding image quality assessment, the SNR and CNR are compared among multiple groups of patients examined in three types of MDCT. In regard to SNR, in our study it is noted that there are no significant differences among brain groups and chest groups according to the three multi-detector rows of 16-MDCT, 32-MDCT, and 64-MDCT. Where, the determined means of SNR and P-value of brain groups are (11.5 ± 1.35 , 11.75 ± 4.13 , 12.3 ± 5.61 , and 0.9) and for chest While, the determined means of SNR and P-value of chest groups are (3.83 ± 0.76 , 4.18 ± 1.35 , 5.92 ± 3.1 , and 0.05) respectively. **Conclusion:** The mean value of radiation doses (CTDI_v in mGy, DLP in mGy.cm and ED in mSv) higher in 64 than 32 and less than that in 16 in chest and brain CT scan. While the image quality was higher in higher CT multi-detector rows, it is non-significant in chest and brain CT exam.

Keywords

Multi-detector CT scan, Radiation dose, Image quality, Contrast to Noise Ratio, Signal to Noise Ratio.

Comparing MDCT systems to traditional single slice CT systems, they have significantly better diagnostic capabilities. These systems were created, are currently utilized more frequently than ever, and development has

advanced far more quickly than the majority of physicians had predicted (1).

There are several other names for this method, including multi-detector CT (MDCT), multi-detector

row computed tomography (MDCT), multi-channel CT, multi-slice CT (MSCT), and multi-detector array helical CT. The number of the concurrent, yet independent measurements that have been taken along the long axis of the patient has been termed as "slices" (2).

The 3rd-generation CT geometry, which is used by MDCT scanners, rotates both detector arc and x-ray tube concurrently. All of the MDCT scanners include slip-ring gantry, allowing for helical acquisition at rotational speeds as quick as 0.33sec for a full 360° rotation of X-ray tube around the patient. The Elscint CT Twin, a scanner that has 2 rows of detectors, was available since 1992, and in 1998, numerous manufacturers began offering MDCT scanners with 4 detector rows. Those scanners' key benefit is their ability to scan multiple slices at once, which enables them to utilize X-ray tube's energy more effectively. The time that is needed for scanning a particular volume could be greatly decreased. Each one of the axial rotations now records additional slices, or data channels, with the 64-detector systems becoming more widespread (3).

With the MDCT scanners, thinner slices could be utilized for the purpose of covering some certain anatomic volume. Which significantly improves spatial resolution while avoiding the disadvantage of greater scan times in longitudinal directions. Enhanced longitudinal resolution has a significant positive impact on 3D representations as well as multi-planar reformatting (MPR, perpendicular or oblique to trans-axial plane). The most popular mode of the scan acquisition in the MDCT is the spiral scanning because it effectively reduces total scan time through continuous acquisition of the data and overlapping datasets, enabling the reconstruction of improved multi-planar reconstruction (MPR) and 3D images without subjecting the patient to additional radiation doses (2,4).

Thin slices are scanned, yielding a single data set that, based on the thickness regarding the reconstructed slice, could be used to produce images with either standard or high longitudinal resolution. One scan series (standard + high-resolution) is adequate for chest exams instead of two. Coronal, axial, and oblique images regarding face bone and the sinuses could be created through secondary reformation utilizing same set of the spiral MDCT scan data (5).

Image quality in CT scanning is a wide concept. It might include a range of radiation dosage-related

traits, like the ones that modify exposure. Certain image quality aspects, like the motion artifacts, are unrelated to patient dosage. Image contrast and image noise have been considered as the most pertinent characteristics of the image quality once those motion artifacts have been removed. Quantum mottle or image noise is most closely connected to radiation dosage that has been utilized for the CT scans. In the case when the dose of the radiation is raised, noise is frequently decreased and vice versa. To minimize radiation dose and improve image quality, one can calculate image noise using standard deviation regarding CT number (in Hounsfield units). For the purpose of finding lesions of low contrast that might be concealed by more pronounced image noise levels, picture noise is very important. At the same time, because the lesion-to-background contrast in studies like CT colonography, chest CT, and kidney stone protocol CT is superior, higher noise levels could be tolerated in these types of studies in order to lower radiation exposure (6).

Dosage and image quality evaluation are significantly impacted by the variety of CT scanners (low-multislice CT (2-16), spiral CT, axial CT, and high-multislice CT (32-64) and imaging methods that are utilized in the CT (7).

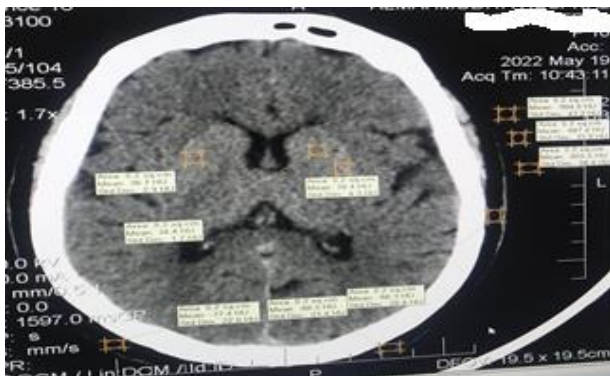
Patients and Methods

The presented work was conducted on (60) consecutive patients being examined by a CT scan from (March 2022) to (August 2022), with patients varying ages from (18 to 70 years). The work in the study was done in Baghdad. The experiments were carried out on three different multiple slices computed tomography (MSCT) scanners (16 slice PHILIPS & SIEMENS), (32 slice SIEMENS) and (64 slice TOSHIBA & SIEMENS). The primary scan parameters that may be modified by technicians or operators are kVp and mAs, which have a substantial influence on picture quality and radiation exposure to the patients. In this study the protocol used (120 kVp, automatic modulation mAs). Dose information was obtained from the protocols designated for each device, and DLP and CTDI_v were calculated. CTDI_{vol} measures exposure per tissue slice over the whole scan duration, assuming no gaps or overlapping in the scan slices. There is a direct relationship

between CTDI_{vol} and pitch parameter (8). Using DLP, CT radiation exposure is measured. The difference between (CTDI_{vol}) and (DLP) is that CTDI_{vol} reflects the dosage as an appropriate scan slice. DLP measures radiation output length along a patient's long axis. It determines total exposure for a set of the scans. It may be estimated in the case where irradiated volume length (i.e. length of the Scan) and the CTDI_{vol} are known by the use of the following equation (9):

$$DLP = CTDI_{vol} \times \text{Scan length.}$$

According to this equation, if the scan duration is extended, the DLP will rise as well. Although the DLP more accurately represents the radiation dosage for a particular CT test, variations in patient anatomy influence its value. For that, CTDI_{vol} is recovered



instrument for comparing radiation doses among procedures.

Effective dose calculations need specific knowledge of unique scanner features, the relationship may be used to provide a good estimate of effective dosage regardless of scanner type (8).

$$\text{Effective Dose} = k \cdot DLP$$

where k values (0.0023 and 0.017) is a weight factor in (mSv/mGy cm) which has been mainly determined by the body regions (Head and Chest) respectively (10).

On E film workstation, the images have been viewed. Images in the axial plane have been used to reconstruct each image at a thickness of 5.0 mm. For the aorta and basal ganglia in the chest and brain tests, respectively, standardized (2) mm-diameter circular regions of interest (ROIs) representing value of mean attenuation and SD in the Hounsfield units (HU) were employed to record signal and noise (11).

$$CNR = \frac{HU_{\text{Target}} - HU_{\text{BG air}}}{SD_{\text{BG air}}}$$

$$SNR = \frac{HU_{\text{Target}}}{SD_{\text{Target}}}$$

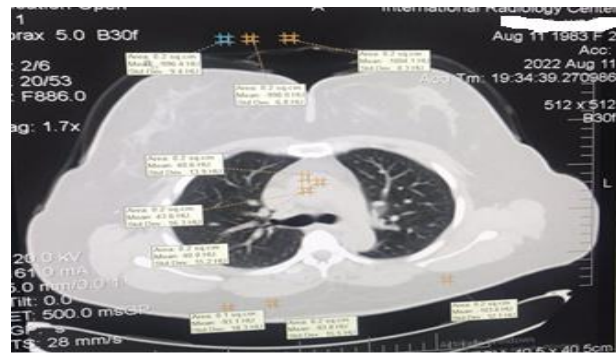


Figure 1: The values of standard deviation (SD) and Hounsfield units (HU) for the aorta in the chest examinations.

Figure 2: The values of standard deviation (SD) and Hounsfield units (HU) for the basal ganglia in the brain examinations.

The CNR, which assesses the contrast between the background and the tissue of interest in a medical image, measures this contrast. The SNR measures the ratio of a region's image signal to its background. The ability to visualize objects in a noisy background is affected by the size and contrast of the objects (11).

Statistical Analysis in Methods

The collected data was entered, double checked and analysed using IBM SPSS software version 26. Descriptive statistics that qualitatively summarized the characteristics of the collected data were used in this study. Additionally, ANOVA test was used to determine the significance among study's groups (abdomen, chest, and brain) to their sub-groups of multi-detector rows of CT scan (16-MDCT, 32-MDCT, and 64-MDCT). Furthermore, the utilized p-value that indicates the differences among study's groups, was suggested to be less than 0.05 in this study.

Results

A total of 60 of two equally collected group samples were investigated radiographically for two body parts of brain and chest. In chest examination, the mean value of radiation doses (CTDI_{vol} in mGy, DLP in mGy.cm and ED in mSv) to patients from the 64-slice scanner was the higher as they found to be (12.6±0.21, 478.6±73.3 and 6.7±1.026) respectively. In the case of 32 slice scanner, it was found to be (9.34±0.23, 341.86±11.56 and 4.78±0.164) respectively, which is

lower than the values obtained in 64 slice scanner. The lowest values of radiation doses were found to be (7.6±1.5, 247.9±52.6 and 3.46±0.738) in 16 slice scanners respectively, as listed in Table 1. And in brain scan the mean value of radiation doses (CTDIv in mGy, DLP in mGy.cm, and ED in mSv) to patients from the 64-slice scanner was the higher as they found to be (79.75±1.69, 1598.8±110.8 and 3.35±0.23) respectively. In the case of 32 slice scanner, it was found

to be (69.54±4.74, 986.9±72.17 and 2.07±0.15) respectively, which is lower than the values obtained in 64 slice scanner. The lowest values of radiation doses were found to be (54.21, 943.8±21.74, and 1.98±0.045) in 16 slice scanners respectively, as listed in Table 2. Figure 3,4 indicate how the (DLP in mGy.cm, CTDIV in mGy, and ED in mSv) are considerably different among groups of the chest and brain respectively.

Table 1: Mean value of radiation dose among the study groups examined by 16, 32, and 64MDCT in Chest examination.

	Measures	Study Groups (Means ± SD)			P-value
		16 (n=10)	32 (n=10)	64 (n=10)	
Chest	CTDLV in mGy	7.6±1.5	9.34±0.23	12.6±0.21	<0.001
	DLP in mGy.cm	247.9±52.6	341.86±11.56	478.6±73.3	<0.001
	Effective dose in mSv	3.46±0.738	4.78±0.164	6.7±1.026	<0.001

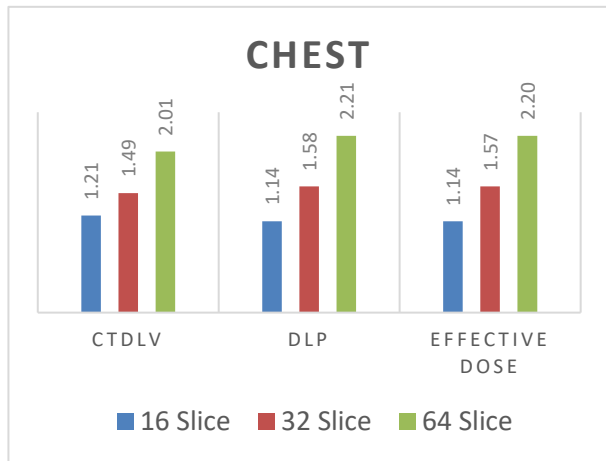


Figure3: Normalized means of CTDLV, DLP, and Effective dose of chest diagnosis.

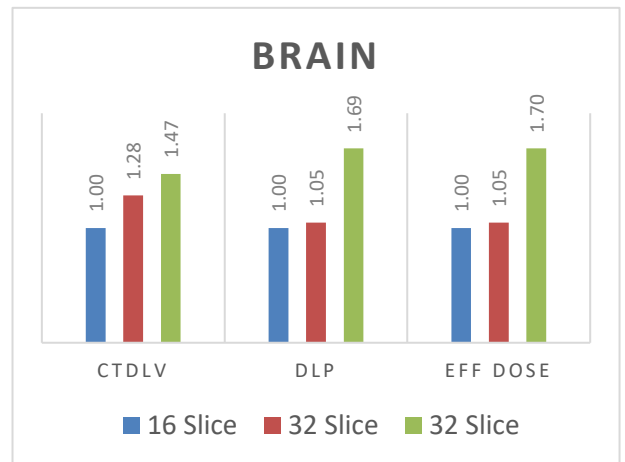


Figure 4: Normalized means of CTDLV, DLP, and Effective dose of brain diagnosis.

Table 2: Mean value of radiation dose among the study groups examined by 16, 32, and 64 MDCT in Brain examination.

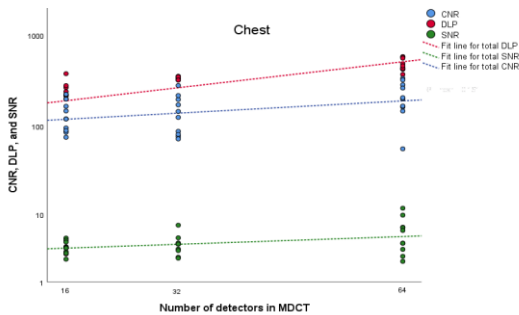
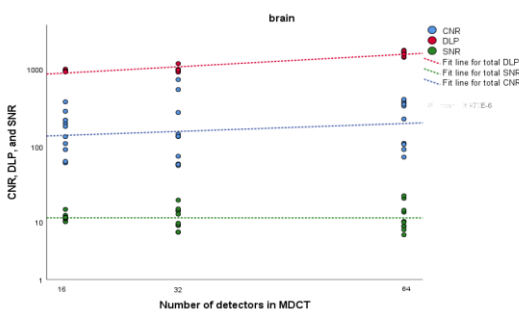
	Measures	Study Groups (Means ± SD)			P-value
		16 (n=10)	32 (n=10)	64 (n=10)	
Brain	CTDLV in mGy	54.21	69.54±4.74	79.75±1.69	<0.001
	DLP in mGy.cm	943.8±21.74	986.9±72.17	1598.8±110.8	<0.001
	Effective dose in mSv	1.98±0.045	2.07±0.15	3.35±0.23	<0.001

Concerning SNR and CNR, it is noted that there are no significant differences among brain groups and chest groups according to the three multi-detector rows of 16-MDCT, 32-MDCT, and 64-MDCT. Where, the determined means of SNR and P-value of brain groups are (11.5±1.35, 11.75±4.13, 12.3±5.61, and 0.9) respectively and mean of CNR and P-value of brain

groups are (173.4±102.8, 222.5±233.9, 246.4±138.2, and 0.6) respectively. While the determined means of SNR and P-value of chest groups are (3.83±0.76, 4.18±1.35, 5.92±3.1, and 0.05) respectively and mean of CNR and P-value of chest groups are (133±50.9, 146.3±71, 215.8±87.9, and 0.03) respectively, as listed in Table 3.

Table3: ANOVA Test of SNR and CNR among CT detectors 16, 32, and 64.

	Measures	Study Groups (Means \pm SD)			P-value
		16 (n=20)	32 (n=20)	64 (n=20)	
Chest	SNR	3.83 \pm 0.76	4.18 \pm 1.35	5.92 \pm 3.1	0.05
	CNR	133 \pm 50.9	146.3 \pm 71	215.8 \pm 87.9	0.034
Brain	SNR	11.5 \pm 1.35	11.75 \pm 4.13	12.3 \pm 5.61	0.9
	CNR	173.4 \pm 102.8	222.5 \pm 233.9	246.4 \pm 138.2	0.617

**Figure5:** Scatter plot of DLP, SNR and CNR as a function of MDCT for chest including data fitting of total DLP, SNR and CNR as a coloured line.**Figure6:** Scatter plot of DLP, SNR and CNR as a function of MDCT for brain including data fitting of total DLP, SNR and CNR as a coloured line.

Discussion

Due to the extensive usage of MDCT, the radiation dose is a source of concern, and the population's total radiation problem is growing. Better quality of the image necessitates a higher dosage of radiation, due to the fact that it contains small gaps of sampling. This highlights an intricate connection between the dose reduction and the quality of the image (12).

This work's objectives were estimating the typical CT dosage descriptors, such as DLP, ED and CTDI_v, and evaluating image quality metrics in the non-contrast chest, abdomen, and brain computed tomography scans that are performed in several hospitals by using various MDCT scanners.

CT images were obtained by three kinds of MDCT

scan with a fixed tube voltage of 120 kV and automatic modulation mAs for the patients who have standard body size. Three different slices were studied (16, 32 and 64 slices).

The CT dose index was first introduced by Shope & Gagne et al. (1981) (13) as metric for measuring the output of the radiation from an examination of the computed tomography that includes several contiguous CT scans (i.e. several adjacent transverse rotations regarding x-ray tube along longitudinal axis of a patient), which can't be evaluated by the conventional procedures of the dosimetry. In order to reflect the average dose to a cylindrical phantom in the core region of a series of scans, the CTDI approach set out to develop an index. One of the derivatives of CTDI_{vol} is DLP. CTDI and the irradiation scan length combine to form DLP. This enables direct comparison of the dosage of the radiation among scanners from various manufacturers and at various scanning parameter settings. CT dose index, on the other hand, doesn't represent the exact dosage for any specific patient; rather, it represents a dose index as it has been determined and estimated in a polymethylmethacrylate phantom.

Even though CTDI is one of the useful tools for comparing protocols, patient-associated factors including shape, size, and inhomogeneous composition are not taken into account. To calculate the absorbed dose, the dose index and patient size can be combined. The patient's attenuation (in other words, the greater the attenuation of the patient, the smaller the dosage of the patient) and size affect patient's dosage for any given scanning method. As a result, the indicated CTDI is lower than the actual dosage that is given to the infants and young children. Using a 100mm pencil-sized chamber of ionization, the CTDI is currently frequently determined after 1 axial scanner rotation. Two-thirds of the peripheral value and 1/3 of central value are added together to get an average (weighted) CTDI. Weighted CTDI must be rectified by pitch factor (dosage index divided by the pitch) when scanning with a pitch that isn't equal to 1, after which it is referred to as volume

CTDI. Dose-Length Product (DLP) A CT scan's total integrated radiation dose is indicated by the DLP, as its name suggests. $DLP = \text{volume CTDI total scan length}$ (in centimeters) comprises both the scan width and the number of scans. The mGy.cm is the unit. The total sum of all section collimations determines the scan length for conventional (non-spiral) scanning; for high-resolution CT, this is 25 mm (25×1 mm).

In this research, we discovered the mean radiation doses (CTDI_v in mGy, ED in mSv and DLP in mGy.cm). The CTDI_{vol} of the chest is higher for slices 16 (7.6 ± 1.5 mGy) than it is for slices 32 (9.34 ± 0.23 mGy) or slices 64 (12.6 ± 0.21 mGy). Additionally, the DLP for the chest 16 slices is (247 ± 52.6 mGy.cm) and is greater in the 64 slices (478.6 ± 73.3 mGy.cm) and 32 slices (341.86 ± 11.56 mGy.cm). Our measured CTDI_{vol} and DLP show significant variations between the 64 slices and 16 slices.

A similar difference was seen in the case of brain also, the CTDI_{vol} of brain for slices 16 is (54.21 ± 0.0 mGy) is higher in 32 slices (69.54 ± 4.74 mGy) while higher in 64 slices (79.75 ± 1.69). And the DLP for the brain 16 slices is (943.8 ± 21.74 mGy.cm) is higher in 32 slices (986.9 ± 72.17 mGy.cm) while higher in 64 slices (1598.8 ± 110.8). Really it is big differences between the 16 slices and 64 slices in our measured CTDI_{vol} and DLP.

The findings in this work were agreed with a recent study performed by Abuzaid & Elshami *et al.* (2021) (14) used different multidetector CT scanners, the 4-, 16- and 160-slice for the routine imaging of the brain in terms of the doses of radiation and image quality, finding dose values 160-slice MDCT were significantly greater dose values for 4- and 16-slice units. And it was compatible with result of Al Ewaidat & Zheng *et al.* (2018) (15) conducted a study that compared the dose of radiation of 16, 32, and 64 slice multidetector computed tomography (MDCT) for brain, chest and abdomen and had noticed that the 64 slice MSCT results in causing higher radiation dosage than the 16, and 32 slice MSCTs. This finding is similar to the findings of Pera & Girjoaba *et al.* (2016) (16) and Karim & Hashim *et al.* (2016) (17), who conducted studies for comparing the dose of the radiation between 2, 4, 16, 32, and 64 slice MSCTs for the brain, abdomen and chest and had noticed that the 64 slice MSCT leads to causing higher radiation dose than all the other MSCT. However, Jaffe & Yoshizumi *et al.* (2009) (18) and Al-zimami (2014) (19) studied radiation doses of 16 and 64 slice devices

and have found that the 64-slice radiation dose is lower compared to the radiation dose of the 16 slices. It might be that such difference is due to differences in protocols used by these studies.

This difference has also been reported between research and it could be related to geometry of the beam differences between the different multidetector CT scanners.

The mean effective dosage for the chest and brain in this work was computed and was found to be 3-6.7 mSv and 1-3.35 mSv, respectively. In comparison to the other works selected for this analysis, effective dosage for brain and chest is significantly lower. Diagnostic CT's allowable dose range is 2-20 mSv (Rawashdeh & Saade *et al.* 2023) (20).

The effective dose as assessed is therefore within the acceptable range. However, even if it is higher than in the other works, the effective dose to the head is still within the permitted dose range. The method utilized might be to blame for this rise in the effective dose of brain. Brain CTDI_{vol} is 3.8% higher in the USA (Satharasinghe & Jeyasugiththan *et al.* 2021) (21), 15% lower in Canada, 19% higher in Malta (Amaoui & Semghouli *et al.* 2019) (22), 3.6% lower in Switzerland (Adam 2019) (23), and 13.9% lower in the UK.

In this study the image quality assessment done quantitatively by comparison between the different MDCT scanners at two regions brain and chest by measurement of CNR and SNR, both parameters were used in many studies for same purpose (Yoon & Kim *et al.*, 2021)(24) in his study on assessment of pediatric CT scan at chest and abdomen he depend on the quantitative evaluation of his result on CNR and SNR, the same parameter used by (Yan *et al.*, 2016)(25) the study depend on 4 parameters in assessment of PET image quality SNR, CNR, bias and image noise. The radiation dose to the slice volume is substantially higher because good contrast resolution needs a high SNR during CT acquisition (Summerlin & Willis *et al.* 2022) (26).

Assessment of the CNR shows that the measurements were higher at 64 slice MDCT in all regions although this result was not significant statistically at brain region and it was significant at chest although P value was border line (0.03).

In regard to SNR, in our study it is noted that there are no significant differences among brain groups and chest groups according to the three multi-detector rows of 16-MDCT, 32-MDCT, and 64-MDCT. Where, the

determined means of SNR and P-value of brain groups are $(11.5 \pm 1.35, 11.75 \pm 4.13, 12.3 \pm 5.61, \text{ and } 0.9)$ and for chest While, the determined means of SNR and P-value of chest groups are $(3.83 \pm 0.76, 4.18 \pm 1.35, 5.92 \pm 3.1, \text{ and } 0.05)$ respectively.

Conclusion

The mean value of radiation doses (CTDIv in mGy, DLP in mGy.cm and ED in mSv) higher in 64 than 32 and less than that in 16 in abdominal, chest and brain CT scan. The Image quality was higher in higher CT multi-detector rows, but it is non-significant in chest and brain CT exam. There are no significant differences of CNR among brain groups and chest groups according to the three multi-detector rows of 16-MDCT, 32-MDCT, and 64-MDCT. The dose of radiation was within the international limit of radiation doses in all MDCT scanners.

References

- Ibad, H.A., de Cesar Netto, C., Shakoor, D., Sisniega, A., Liu, S.Z., Siewerdsen, J.H., Carrino, J.A., Zbijewski, W. and Demehri, S., 2023. Computed tomography: state-of-The-art advancements in musculoskeletal imaging. *Investigative radiology*, 58(1), pp.99-110.
- Khalid, H., Hussain, M., Al Ghamdi, M.A., Khalid, T., Khalid, K., Khan, M.A., Fatima, K., Masood, K., Almotiri, S.H., Farooq, M.S. and Ahmed, A., 2020. A comparative systematic literature review on knee bone reports from mri, x-rays and ct scans using deep learning and machine learning methodologies. *Diagnostics*, 10(8), p.518.
- Alghairi, M., Sulaiman, N. and Mutashar, S., 2020. Health care monitoring and treatment for coronary artery diseases: challenges and issues. *Sensors*, 20(15), p.4303.
- Jung, H., 2021. Basic physical principles and clinical applications of computed tomography. *Progress in Medical Physics*, 32(1), pp.1-17.
- Seeram, E., 2018. Computed tomography: a technical review. *Radiologic technology*, 89(3), pp.279CT-302CT.
- Serrell, E.C. and Best, S.L., 2022. Imaging in stone diagnosis and surgical planning. *Current Opinion in Urology*, 32(4), pp.397-404.
- Nakamura, Y., Higaki, T., Tatsugami, F., Honda, Y., Narita, K., Akagi, M. and Awai, K., 2020. Possibility of deep learning in medical imaging focusing improvement of computed tomography image quality. *Journal of computer assisted tomography*, 44(2), pp.161-167.
- Abdalla, M.A.M., 2019. *Evaluation of Patient Effective Dose and Organ Dose during Chest Computed Tomography* (Doctoral dissertation, Sudan University of Science and Technology).
- Romans, L., 2018. *Computed Tomography for Technologists: A comprehensive text*. Lippincott Williams & Wilkins.
- MeÅ, N., 2021. COMPARISON OF IMAGE QUALITY AND DIFFERENT RADIATION DOSES IN COMPUTERIZED TOMOGRAPHIC DIAGNOSTICS. *Acta Medica Saliniana*, 50(1-2).
- McCullough, C.H. and Schueler, B.A., 2000. Calculation of effective dose. *Medical physics*, 27(5), pp.828-837.
- Furlow, B., 2010. Radiation dose in computed tomography. *Radiologic technology*, 81(5), pp.437-450.
- Shope, T.B., Gagne, R.M. and Johnson, G.C., 1981. A method for describing the doses delivered by transmission x-ray computed tomography. *Medical physics*, 8(4), pp.488-495.
- Abuzaid, M.M., Elshami, W., Tekin, H.O., Sulieman, A. and Bradley, D.A., 2021. Comparison of Radiation dose and Image Quality in Head CT Scans Among Multidetector CT Scanners. *Radiation protection dosimetry*, 196(1-2), pp.10-16.
- Al Ewaidat, H., Zheng, X., Khader, Y., Abdelrahman, M., Alhasan, M.K.M., Rawashdeh, M.A., Al Mousa, D.S. and Alawneh, K.Z.A., 2018. Assessment of radiation dose and image quality of multidetector computed tomography. *Iranian Journal of Radiology*, 15(3).
- Pera, C.M., Girjoaba, O.I., Cucu, A. and Iosif, M., 2016. Comparison of radiation dose in abdomen-pelvis and trunk imaging between 64 slice and 16 slice CT. *Physica Medica*, 32, p.295.
- Karim, M.K.A., Hashim, S., Sabarudin, A., Bradley, D.A. and Bahrudin, N.A., 2016. Evaluating organ dose and radiation risk of routine CT examinations in Johor Malaysia. *Sains Malaysiana*, 45(4), pp.567-573.
- Jaffe, T.A., Yoshizumi, T.T., Toncheva, G., Anderson-Evans, C., Lowry, C., Miller, C.M., Nelson, R.C. and Ravin, C.E., 2009. Radiation dose for body CT protocols: variability of scanners at one institution. *American Journal of Roentgenology*, 193(4), pp.1141-1147.
- Alzimami, K., 2014. Assessment of radiation doses to paediatric patients in computed tomography procedures. *Polish journal of radiology*, 79, p.344.
- Rawashdeh, M., Saade, C., Al Mousa, D.S., Abdelrahman, M., Kumar, P. and McEntee, M., 2023. A new approach to dose reference levels in pediatric CT: Age and size-specific dose estimation. *Radiation Physics and Chemistry*, 205, p.110698.
- Satharasinghe, D.M., Jeyasinghtham, J., Wanninayake, W.M.N.M.B. and Pallewatte, A.S., 2021. Paediatric diagnostic reference levels in computed tomography: a systematic review. *Journal of Radiological Protection*, 41(1), p.R1.
- Amaoui, B., Semghouli, S., Massaqa, M., Aabid, M., Hakam, O.K., Choukri, A. and El Kharras, A., 2019. Radiation Doses from Computed Tomography Practice in Regional Hospital Center Hassan II of Agadir, Morocco. *Indian Journal of Public Health Research & Development*, 10(10).
- Adam, A.H.Y., 2019. *Assessment of Radiation Dose to Head, Chest and Abdomen of Adult Patients Underwent Computed Tomography Examination-Khartoum State-Sudan* (Doctoral dissertation, Sudan University of Science and Technology).
- Yoon, H., Kim, J., Lim, H.J. and Lee, M.J., 2021. Image quality assessment of pediatric chest and abdomen CT by deep learning reconstruction. *BMC medical imaging*, 21(1), pp.1-11.
- Yan, J., Schaefferkoetter, J., Conti, M. and Townsend, D., 2016. A method to assess image quality for low-dose PET: analysis of SNR, CNR, bias and image noise. *Cancer Imaging*, 16(1), pp.1-12.
- Summerlin, D., Willis, J., Boggs, R., Johnson, L.M. and Porter, K.K., 2022. Radiation Dose Reduction Opportunities in Vascular Imaging. *Tomography*, 8(5), pp.2618-2638.